"This is the peer reviewed version of the following article: [Structural Control and Health Monitoring] *which has been published in final form at* [https://onlinelibrary.wiley.com/doi/10.1002/stc.2798] *purposes in accordance with Wiley Terms and Conditions for Self-Archiving."*

A simplified design method of tuned inerter damper for damped civil structures: theory, validation, and application

Tiancheng Xu[1], Yancheng Li[1,2], Tao Lai[1] and Jiajia Zheng[3]

Abstract

This paper reports an analytical method to obtain approximate solution for optimal design of tuned inerter damper (TID) in MDOF damped civil structures. The method is based on the equivalent linearization method which converts the mass-stiffness-damping system into a mass-equivalent stiffness system and a technique which converts a modal subsystem of MDOF structure-TID system into a equivalent SDOF system. The solution and procedures for optimal design of SDOF and MDOF systems are introduced. Following this, the proposed method is verified through comparison with the numerical search methods for SDOF system. A case study of optimal TID design for a MDOF system is given and the results show that the proposed method is able to find the optimal damping ratio and tuning ratio of the TID to minimize the structural response.

Keywords: Tuned inerter damper; Optimal design; The equivalent linearization method; MDOF structures; Structural control; Damped structures;

1 Introduction

Unwanted structural vibrations induced by natural hazard such as the earthquake and wind loads are recognized as serious safety concern. The passive vibration control technique is widely used to suppress the undesirable structural responses due to the low maintenance cost and high reliability. Recently, a new form of passive vibration control device, i.e., inertance device, has drawn attention in civil engineering community to enhance the structural performance under external dynamic events. Inerter, invented by Smith [1], is a two-terminal device in which the force produced on the terminal is proportional to the acceleration difference between the two ends, and the proportional constant is called inertance. The main advantage of inerter is its ability in offering mass amplification effect as it can generate an apparent mass hundreds of times higher than the actual mass. Ever since inerter was invented, it has been proposed to employ in many engineering applications for effective vibration control and mitigation, e.g., formula one car [2], vehicle suspension systems [3], the train suspension systems [4], the semisubmersible platform [5] and many others [6-7].

For civil engineering applications, various inerter based devices have been proposed due to its great potentials [8]. In [9-10] an inerter-based vibration mitigation device called tuned viscous mass dampers (TVMD) is proposed for seismic control of building and a shake table test with earthquake excitation verified the effectiveness of the TVMD. Tuned-mass-damper-inerter (TMDI) is another promising passive structural control device, in which an inerter is connected to the mass element of the traditional tuned-mass-damper (TMD) in series. It was presented by Marian and Giaralis in [11] as a generalization of the traditional TMD and the numerical application indicates that the use of inerter element can effectively enhance the performance of TMD due to the mass amplification effect. Several studies [12-13] have investigated the optimization and application of TMDI in many cases and also confirmed that the inerter can provide considerable additional mass to increase the original mass of TMD.

In this context, Lazar et al. [14] proposed a novel inerter-based passive control system to suppress vibration in civil structures, namely the tuned-inerter-damper (TID). It is a system including inerter connected in-series to a parallel assembled spring and dashpot, similar to the TMD structurally with the mass element replaced by the inerter. The TID should be located between adjacent storeys because inerter is a two-terminal device. Through modal analysis, Lazar found that for best performance the TID should be located at bottom storey where the primary structure is subjected to base excitation. Due to the small size of inerter, the novel TID system takes advantage of compact configuration and being convenient and economical to implement compared to TMD.

There are a large number of existing studies [15][16] that examined the optimal design and control performance of TID. In vehicle suspension, Shen et al. [17] used the TID to reduce the acceleration of car body and improve the vehicle driving comfort. In cable vibration control, several studies [18-19] investigated the optimal installation site of TID in cable, the performances of inerter-based and non-inerter-based devices were compared. Nevertheless, majority of the ongoing research on the TID is in the seismic control of civil structures. In [20] the closed-form solution for TID in building isolation under H_2 optimization criterion was derived. Domenicao et al. recently reported a study of TID in combination

with base isolated structures[21], the results indicate that the TID can reduce the response of base isolated structures thus protect the structure from harmful base motion. Krenk and Høgsberg [22] have designed the TID focusing on the attenuation of non-resonant modes to improve the structural performance.

For most passive control devices, the key point of system design is to collectively choose the appropriate parameters to achieve optimal performance. There are three design parameters in TID system, i.e., the inertance-mass ratio (ratio of the TID inertance to the primary structural mass), the tuning ratio (ratio of the TID natural frequency to the natural frequency of the primary structure) and the TID damping ratio. Because the inertance-mass ratio is often fixed and limited, thus the main design parameters of TID are its tuning ratio and damping ratio. Up to now, there exists several approaches in the literature regarding the optimal design of TID. In [14], Lazar proposed a straightforward numerical approach to obtain the optimal tuning ratio and damping ratio of TID considering an undamped structure subjected to base excitation. The optimization rules are based on fixed-point theory established by Den Hartog for an undamped single-degree-of-freedom (SDOF) main structure. Hu et al. [23] derived the analytical solution of TID in both H_∞ and H_2 criterion considering an undamped SDOF primary structure. In [24], Shen et al. derived two sets of analytical formula for optimal deign of TID based on the fixed-point theory for undamped SDOF structure. For general case, i.e., the primary is damped, Wen et al. [25] have use multiple TIDs to control the seismic response of damped multi-DOF structure. The location and mode for tuning of the multi-TIDs were determined by numerical procedure. In [26], Pan and Zhang designed the TID with the response mitigation ratio approach considering a damped SDOF structure. The optimal parameters were determined numerically and then the results were fitted into a set of empirical formula. In summary, for simple undamped SDOF structure, there are a number of approaches available for optimal design of TID and even the closed-form design formula had been derived. However for damped structures, it is still a challenge to obtain such closed-form solution of design parameters while only a numerical approach [25] or empirical fitting formula [26] have been provided until now. This may be due to the fact that the system equations are too complex to calculate analytically when there is damping in the primary structure. For instance, there is no longer any fixed point when carrying out the optimization procedure if the primary structure is damped. Although these numerical procedures can obtain the design parameters with satisfactory performance, the procedures maybe computationally inefficient or not convenient to be applied practically.

However, all real engineering systems have inherent damping. To address this issue, a simplified engineering design approach should be developed. In this paper, the optimal design of TID system in H_2 criterion for both damped SDOF and MDOF structures is achieved via a simple and convenient analytical formula. Design approach is proposed for optimal performance of damped structure as well. The analytical approach is based on the equivalent linearization method [27-28] considering the response of nonlinear system to random excitation. This method has been used extensively as an approximate analytical method [29-30] in optimal design of structures with TMDs. The principle of equivalent linearization method is to construct a linear oscillator to replace the original nonlinear one subjected to same excitation. In [31-32], Anh and Nguyen first extended the principle of equivalent linearization method to design TMD for SDOF damped structure. They replaced the original damped structure by an equivalent undamped structure and used the classical Den Hartog tuning formula to obtain the optimal tuning ratio of TMD. The final expression is simple and accurate but the formula of optimal damping ratio of TMD cannot be obtained. Here we improve the equivalent linearization method so that it can analytically obtain both optimal tuning ratio and damping ratio of TID for damped structure. The accuracy of analytical solutions is validated by comparing with proven numerical optimization approaches.

In a word, the original contribution of this paper is that: (i) For damped SDOF structures, it improves the equivalent linearization method such that it can obtained the analytical solutions of optimal damping ratio of TID except for the optimal tuning ratio; (ii) For MDOF structures, first the relation between modal response and installation location of TID is investigated. Then the optimal installation location and additional modal damping ratio provided by TID can be determined accurately. Based on these above, a simple analytical design approach of TID for MDOF damped structure is proposed. This paper has been divided into four parts and begins with the principle of improved equivalent linearization method and a practical design procedure in H_2 criterion. It continues in modal analysis of MDOF structure-TID system and proposing the simple design procedure of TID for MDOF structure. Then the accuracy of analytical solutions by equivalent linearization method is verified by comparing with the numerical exact solutions in section 4. Finally, a case study with a MDOF structure-TID system subjected to both harmonic and seismic excitation is performed to demonstrate the efficiency of the proposed approach.

2 The simplified design for damped SDOF structure

2.1 The equivalent linearization method

TID is a two-terminal device which consist of an inerter with inertance *b*, a stiffness element k_d, and a damper element c_d as shown in Figure 1. In SDOF structures, TID is installed between the primary structure and the ground (just like the installation of stiffness or damper in Figure 2 (a)). The primary objective of optimal design of TID is to find appropriate stiffness and damping parameters of TID, that is the optimal tuning and damping ratio respectively, to maximize the vibration mitigation of a structure in a given inertance (or apparent mass). It can be seen in following section 2.2 that the explicit analytical solutions of the design problem are readily obtained in case that primary structure is undamped. However it is almost impossible to obtain the explicit analytical solution in the damped case due to the existence of inherent damping greatly increases the difficulty of solving.

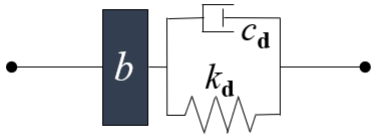

Figure 1 Schematic of the tuned inerter damper

In order to obtain a closed-form expression for optimal tuning ratio and damping ratio in damped case, an improved equivalent linearization method is proposed in this paper. The principle of equivalent linearization method is using an equivalent undamped structure to substitute the damped structure as shown in Figure 2.

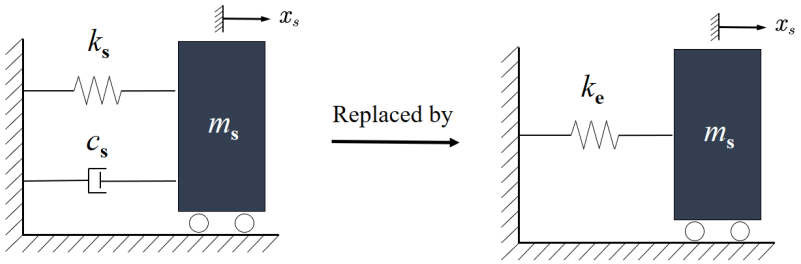

Figure 2 The principle of the equivalent linearization method

The original damped system is shown in Figure 2 (a) and the approximate undamped system is shown in Figure 2 (b). The original damped system consists of primary structure mass m_s, stiffness k_s, damping c_s (notice that the main structure is undamped when $c_s = 0$) and here x_s denotes the displacement of main mass m_s. In Figure 2 (b), the k_e is the equivalent stiffness of the equivalent undamped system and its property is discussed in following.

First following dimensionless parameters are introduced

$$\omega_s = \sqrt{\frac{k_s}{m_s}},\ \omega_d = \sqrt{\frac{k_d}{b}},\ \gamma = \frac{\omega_d}{\omega_s},\ c_{scr} = 2m_s\omega_s,\ c_{dcr} = 2b\omega_d$$

$$\xi_s = \frac{c_s}{c_{scr}},\ \xi_d = \frac{c_d}{c_{dcr}},\ \omega_e = \sqrt{\frac{k_e}{m_s}},\ \hat{\gamma} = \frac{\omega_d}{\omega_e}$$

where ω_s and ω_d are the natural frequencies of original structure (Figure 2 (a)) and TID, respectively. γ is the nondimensional tuning ratio of TID for original damped system. c_{scr} and c_{dcr} are the critical damping coefficients of structure and TID, respectively. $\xi_s = c_s/c_{scr}$ and $\xi_d = c_d/c_{dcr}$ are the nondimensional damping ratios of original structure and TID, respectively. While in the approximate undamped system (Figure 2 (b)), the equivalent natural frequency ω_e is introduced as well as the tuning ratio $\hat{\gamma}$. In order to represent ω_s with respect to ω_e under the criterion proposed in [31], a set of procedures are carried out as follows.

Considering two systems in Figure 2, the equation of motion for damped primary structure can be written as

$$\ddot{x}_s + 2\xi_s \omega_s \dot{x}_s + \omega_s^2 x_s = 0 \tag{1}$$

while for approximate undamped primary structure, the equation of motion is

$$\ddot{x}_s + \omega_e^2 x_s = 0 \tag{2}$$

To make the approximate system equivalent to the original system, we define the error between original system Eq. (1) and approximate undamped system Eq. (2) as $2\xi_s \omega_s \dot{x}_s + \omega_s^2 x_s - \omega_e^2 x_s$. Here we use the mean square error criterion [34] which aims to find ω_e to minimum the mean square error between the two systems as follows

$$I_e = \frac{1}{\Omega}\int_0^{\Omega} (2\xi_s \omega_s \dot{x}_s + \omega_s^2 x_s - \omega_e^2 x_s)^2 dt \tag{3}$$

where Ω is a critical constant determining the accuracy of results and denotes the upper bounds of the integral. Then the values of ω_e are determined by the conditions

$$\frac{\partial I_e}{\partial \omega_e^2} = 0 \tag{4}$$

After a series of calculations and rearranging obtains

$$\omega_e^2 + \frac{1-\cos 2\Omega}{\Omega + \frac{1}{2}\sin 2\Omega}\xi_s \omega_s \omega_e - \omega_s^2 = 0 \tag{5}$$

Then the ω_e can be solved and the solution is

$$\begin{gathered} \omega_e = \frac{\omega_s}{Coe} \\ Coe = \sqrt{1 + \frac{1}{4}\left(\frac{1-\cos 2\Omega}{\Omega + \frac{1}{2}\sin 2\Omega}\right)^2 \xi_s^2} + \frac{1}{2}\frac{1-\cos 2\Omega}{\Omega + \frac{1}{2}\sin 2\Omega}\xi_s \end{gathered} \tag{6}$$

Note that Coe is a converting coefficient from ω_e to ω_s (i.e. $\omega_s = \omega_e \times Coe$) and it is a function of structural damping ratio ξ_s. It means that the equivalent stiffness coefficient k_e is a combination of original structural stiffness k_s and damping c_s.

Consequently, we have the tuning ratio and the equivalent tuning ratio

$$\gamma = \frac{\omega_d}{\omega_s}, \quad \hat{\gamma} = \frac{\omega_d}{\omega_e} \tag{7}$$

It is clear that the ω_s in γ can be represent by ω_e in $\hat{\gamma}$ as the form of Eq. (6). Then we can obtain the tuning ratio of TID for damped structure by substitute the Eq. (6) into Eq. (7) as follow

$$\gamma = \frac{\omega_d}{\omega_s} = \frac{\omega_d}{\omega_e Coe} = \frac{\hat{\gamma}}{Coe} \tag{8}$$

The damping ratio of TID for damped case cannot be obtained by the same method in [31] and [32] because of mathematically there is no ω_s in the expression of ξ_d (i.e. $\xi_d = c_d/2b\omega_d$) and thus we can not to utilize the converting coefficient Coe to transform ξ_d, the damping ratio of TID. Hence here only the optimal tuning ratio is obtained. To this end, we use a newly defined damping ratio of TID, it is

$$\xi_{d_{new}} = \frac{c_d}{c_{scr}} = \frac{c_d}{2m_s\omega_s} \tag{9}$$

While for the approximate undamped structure, the damping ratio of TID is

$$\hat{\xi}_{d_{new}} = \frac{c_d}{2m_s\omega_e} \tag{10}$$

Whereupon the optimal damping ratio of TID for damped structure can be obtained as

$$\xi_{d_{new}} = \frac{c_d}{2m_s\omega_s} = \frac{c_d}{2m_s\omega_e Coe} = \frac{\hat{\xi}_{d_{new}}}{Coe} \tag{11}$$

For convenience, we use ξ_d to represent $\xi_{d_{new}}$ in following paragraph.

Through the above analysis, the equivalent linearization method is based on a pure structure rather than a structure incorporating a specific controller. Thus, the most outstanding advantage of the method is that can be conveniently and succinctly used for any controller in theory. If the analytical solutions for undamped is known, then the explicit analytical solutions for damped case can be obtained by transfer factor Coe directly. However, when the method is applied to a new controller, the effect is not predictable and may need to be adjusted according to different controller. Herein, the effectiveness of the method for TID was examine and an optimization design of TID for damped structure was taken as an example in following.

2.2 Optimization of TID for SDOF structure

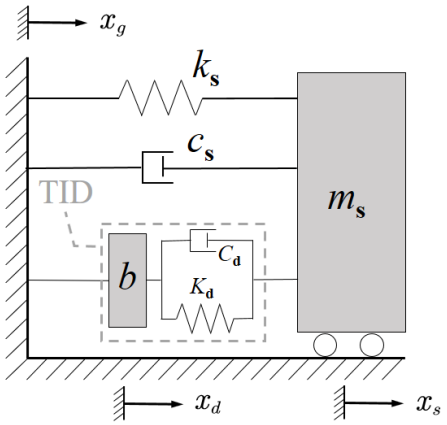

Figure 3 TID-structure system subjected to ground excitation

Firstly, we consider a system with a TID mounted on the damped SDOF structure subjected to ground excitations. Figure 3 shows the system model in which the structural parameters are same as those in Figure 2 (a). The system is subjected to ground displacement x_g with the frequency ω, then the main mass and TID displacements in absolute coordinates are represented as x_s and x_d, respectively.

Now the equations of motion can be written as

$$\begin{aligned} m_s\ddot{x}_s + c_s(\dot{x}_s - \dot{x}_g) + c_d(\dot{x}_s - \dot{x}_d) + k_s(x_s - x_g) + k_d(x_s - x_d) = 0 \\ b(\ddot{x}_d - \ddot{x}_g) + c_d(\dot{x}_d - \dot{x}_s) + k_d(x_d - x_s) = 0 \end{aligned} \tag{12}$$

Meanwhile introduce the dimensionless parameters as follows:

$$\left.\begin{aligned} \mu &= \frac{b}{m_s}\text{:inertance to mass ratio} \\ \lambda &= \frac{\omega}{\omega_s}\text{:excitation frequency ratio} \end{aligned}\right\} \tag{13}$$

By combining the Eq. (12) and Eq. (13), the relation from ground acceleration to absolute acceleration response in Laplace domain can be written as a function with respect to complex variable s, that is

$$TF_{\ddot{x}_s}(s) = \frac{\begin{array}{c}(2\xi_d\mu\omega_s + 2\xi_s\mu\omega_s)s^3 + (\mu^2\omega_d^2 + \mu\omega_s^2 + 4\xi_d\xi_s\omega_s^2)s^2 \\ +(2\xi_s\mu\omega_d^2\omega_s + 2\xi_d\omega_s^3)s + \mu\omega_d^2\omega_s^2\end{array}}{\begin{array}{c}\mu s^4 + (2\xi_d\omega_s + 2\xi_d\mu\omega_s + 2\xi_s\mu\omega_s)s^3 + (\mu^2\omega_d^2 + \mu\omega_d^2 + \mu\omega_s^2 + 4\xi_d\xi_s\omega_s^2)s^2 \\ +(2\xi_s\mu\omega_d^2\omega_s + 2\xi_d\omega_s^3)s + \mu\omega_d^2\omega_s^2\end{array}}. \tag{14}$$

In addition, the one of the original damped structure (i.e. The Figure 2 (a), no TID controlled) is

$$TF_o(s) = \frac{2\omega_s \xi_s s + \omega_s^2}{s^2 + 2\omega_s \xi_s s + \omega_s^2} \tag{15}$$

It should be noted that here the definition of TID damping ratio is different from that of general case, i.e. $\xi_d = c_d / 2b\omega_d$. The reason for that is to associate ξ_d with ω_s so that equivalent linearization method can be used to derive ξ_d.

For optimal design, we use the H_2 optimization since it is more suitable for random excitation such as the earthquake and wind load. The performance index of H_2 optimization is the area of frequency response curve over all frequency ranges namely the total vibration energy of the system subjected to stationary random excitation with a uniform power spectrum density S_o, and is defined as follows:

$$I = \frac{E[\ddot{x}_s^2]}{2\pi S_o \omega_s} \tag{16}$$

where $E[\ddot{x}_s^2]$ is the mean square value of the acceleration response $\ddot{x}_s$ and has the form

$$E[x] = \int_{-\infty}^{\infty} S_o |TF(i\omega)|^2 d\omega = S_o \omega_s \int_{-\infty}^{\infty} |TF(\lambda)|^2 d\lambda \tag{17}$$

where $TF(i\omega)$ is the transfer function $TF(s)$ whose s is replaced by $i\omega$ and $i = \sqrt{-1}$ is the imaginary unit. After substituting Eq. (17) into (16), the index I can be rewritten as

$$I = \frac{1}{2\pi} \int_{-\infty}^{\infty} |TF(\lambda)|^2 d\lambda \tag{18}$$

In practice, it denotes the dimensionless mean-square response of the system under white-noise excitation. Take the transfer function Eq. (15) as an example, the performance index for an original damped SDOF structure without a TID is given by definite integral

$$I_o(\xi_s) = \frac{1}{2\pi} \int_{-\infty}^{\infty} |TF_o(\lambda)|^2 d\lambda = \frac{4\xi_s^2 + 1}{4\xi_s} \tag{19}$$

This equation indicates that the performance index I_o is only relate to structural inherent damping ratio ξ_s. The relation is scrutinized in a Figure 4 with I_o on the y-axial, ξ_s on the x-axial. It indicates that the damping is not the larger the better as the excess damping will restrict its relative motion. For a uncontrolled damped structure, the optimal damping ratio is $\xi_s = 0.5$ which corresponding to the minimum value 1 of I_o.

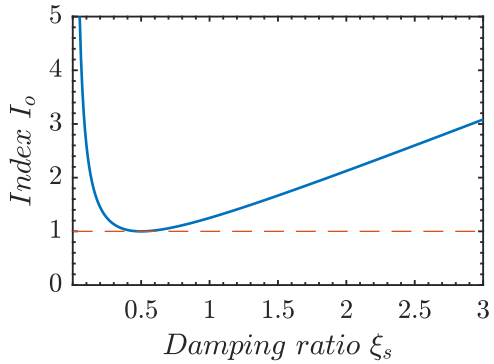

Figure 4 The performance index I_o of original damped structure without a TID against the damping ratio ξ_s.

For TID-structure system shown in Figure 3, the optimal parameters of γ and ξ_d, according to [33], can be found when the first-order partial derivative of performance index I in Eq. (18) with respect to γ and ξ_d both equal to zero, that is

$$\left.\begin{aligned}\frac{\partial I}{\partial \gamma}&=\frac{1}{2\pi}\int_{-\infty}^{\infty}\frac{\partial|TF(\lambda)|^2}{\partial \gamma}d\lambda=0\\ \frac{\partial I}{\partial \xi_d}&=\frac{1}{2\pi}\int_{-\infty}^{\infty}\frac{\partial|TF(\lambda)|^2}{\partial \xi_d}d\lambda=0\end{aligned}\right\} \tag{20}$$

Combining the Eq.(14), and (18), one can obtains the closed-form index I as

$$\begin{aligned}&I(\mu,\gamma,\xi_d,\xi_s)=\\ &\frac{\begin{aligned}&\xi_s\gamma^4\mu^4(4\xi_s^2+\mu\gamma^2+1)+16\xi_s\mu\xi_d^4+(16\xi_s^2\gamma^2\mu^2+32\xi_s^2\mu+16\xi_s^2+4(\mu^2-\mu+1))\xi_d^3\\ &+(4\xi_s\mu(8\xi_s^2\gamma^2\mu+4\xi_s^2\gamma^2+4\xi_s^2+\gamma^4\mu^3+\gamma^4\mu^2-\gamma^2\mu+\gamma^2+2\mu+1))\xi_d^2\\ &+(\mu^2(16\xi_s^4\gamma^2+8\xi_s^2\gamma^4\mu^2+12\xi_s^2\gamma^4\mu+4\xi_s^2\gamma^4-4\xi_s^2\gamma^2+4\xi_s^2+\gamma^4+\gamma^2\mu-2\gamma^2+1))\xi_{\mathrm{d}}\end{aligned}}{\begin{aligned}&(16\xi_s(\mu+1))\xi_d^3+(4\mu(\mu+4\xi_s^2+4\xi_s^2\gamma^2+4\xi_s^2\gamma^2\mu))\xi_d^2\\ &+(4\xi_s\mu^2(4\xi_s^2\gamma^2+\gamma^4\mu^2+2\gamma^4\mu+\gamma^4-2\gamma^2+1))\xi_{\mathrm{d}}+4\xi_s^2\gamma^4\mu^4\end{aligned}}\end{aligned} \tag{21}$$

It emerges that I is a function with μ, γ, ξ_d, ξ_s, but is independent of the excitation frequency ω and the primary structural natural frequency ω_s. After substituting Eq. (21) into (20), one obtains a quite complicated equation set in respect of γ and ξ_d (In fact, the maximum order of γ and ξ_d is ten and six). Thus the analytical solutions of Eq. (20) cannot be solved explicitly and we have to find the optimal design parameters by numerical search technique or approximate analytical method as in [33][34]. In this regard, it is of significance to use equivalent linearization method to obtain the explicit closed-form solutions.

It is also need to obtain exact solutions for the purpose of verification of the equivalent linearization. To obtain the exact solutions, Eq. (21) will be used to derive the numerical search procedure as shown in Appendix A in a later section 4. While for the approximate analytical solutions, according to the process at section 2.1, the optimal design parameters of equivalent undamped system are need to derived first. Substituting the $\xi_{\mathrm{s}}=0$ into Eq. (21), then the I reduces to

$$I(\mu,\gamma,\xi_d)=\frac{\xi_d^3(4\mu^2-4\mu+4)+\xi_{\mathrm{d}}\mu^2(\gamma^2\mu-2\gamma^2+\gamma^4+1)}{4\xi_d^2\mu^2} \tag{22}$$

While the Eq. (20) can be given analytical by

$$\left.\begin{aligned}4\xi_d^2(\mu^2-\mu+1)-\gamma^4\mu^2-\gamma^2\mu^3+2\gamma^2\mu^2-\mu^2=0\\ 2\gamma^2+\mu-2=0\end{aligned}\right\}. \tag{23}$$

First we consider the Eq. (23) as equations with respect to γ^2 and ξ_d^2, then they can be solved readily as follows.

$$\left.\begin{aligned}\gamma^2&=\frac{2-\mu}{2}\\ \xi_d^2&=\frac{\gamma^4\mu^2+\gamma^2\mu^3-2\gamma^2\mu^2+\mu^2}{4(\mu^2-\mu+1)}\end{aligned}\right\} \tag{24}$$

The optimal γ and ξ_d can be derived from the above equation, it follows that.

$$\left.\begin{aligned}\gamma^{opt}=\sqrt{\frac{2-\mu}{2}},\ \xi_d^{opt}=\sqrt{\frac{\mu^3(1-\mu/4)}{4(\mu^2-\mu+1)}},\ \text{when } \mu<2\\ \gamma^{opt}=0,\ \xi_d^{opt}=\sqrt{\frac{\mu^2}{4(\mu^2-\mu+1)}},\ \text{when } \mu\geq 2\end{aligned}\right\} \tag{25}$$

Final the optimal performance index I^{opt} can be derived by substituting Eq. (25) into Eq. (22) as following

$$\left.\begin{aligned} I^{opt} &= \frac{(8-2\mu)\sqrt{\mu^2-\mu+1}}{4\sqrt{\mu(4-\mu)}}, \text{ when } \mu<2 \\ I^{opt} &= \frac{\sqrt{\mu^2-\mu+1}}{\mu}, \text{ when } \mu\geqslant 2 \end{aligned}\right\} \tag{26}$$

Expressing the optimal performance index I^{opt} in a similar form of Eq. (19), one obtains the equivalent damping ratio ξ_{se} which offered by TID for the undamped primary structure. that is

$$\xi_{se}(\mu) = \frac{I^{opt} - \sqrt{(I^{opt})^2 - 1}}{2} \tag{27}$$

Please note that this is only true when $I^{opt} \geqslant 1$ because the performance index of original damped structure cannot less than 1 as shown in Figure 4.

The relation between optimal tuning ratio and damping ratio of TID against interance-mass ratio is plotted in Figure 5 (a). For a larger range of $\mu \in [0:3]$, the optimal tuning ratio γ^{opt} is inversely proportional to μ and declines from 1 as μ increases from 0 to 2. While when $\mu \geqslant 2$, the γ^{opt} cannot be obtained in terms of positive number so it stays at 0. On the contrary, the optimal damping ratio ξ_d^{opt} is in direct proportional to μ and increases from 0. When $\mu \geqslant 2$, it goes down slightly. Figure 5 (b) depicts the variation of optimal performance index against inertance-mass ratio, an important point is that the contribution of TID is equivalent to $\xi_s = 0.5$ when μ equal 0.65 because the $I^{opt} = 1$. The index I declines rapidly as the μ increases from 0 to 0.65 and tends to flatten and stabilizing when μ continues to increase. Overall, the minimum performance index I^{opt} is about 0.85 when $\mu = 1.28$ and the ξ_d^{opt} equal 0.51. This indicate the 0.5 also the optimal damping ratio of TID-structure and the optimal performance index is enhanced from 1 to 0.85.

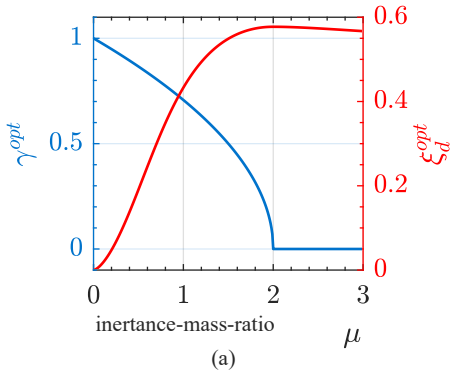

Figure 5 Graphical representation of the optimal design parameters of the TID: (a) left y-axis shows the optimal tuning ratio and right y-axis shows the optimal damping ratio; (b) the optimal performance index.

It is evident that TID will enhance the effort of damper c_d in vibration mitigation. The equivalent damping ratio ξ_e and the actual damper ratio ξ_d^{opt} versus the same μ is plotted in left y-axis of Figure 6 for comparison. The enhancement effect of damper c_d is quantified in terms of magnification times $r_m = \xi_e / \xi_d^{opt}$ and is plotted in right y-axis of the figure. From that it can be seen the enhancement of c_d is considerable when μ or ξ_d^{opt} with a smaller value. While when $\mu \geqslant 0.3$ or $\xi_d^{opt} \geqslant 0.1$, the r_m will fall below 2 and remain around 1.5. In a word, the TID can enhance the beneficial effect of damper and suppress performance degradation due to excessive damping (i.e. $\xi_s > 0.5$).

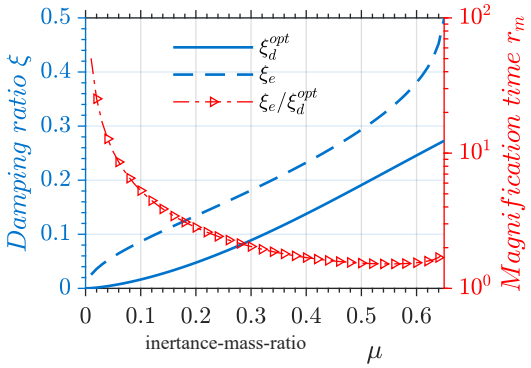

Figure 6 The damping enhance ability of TID; left y-axis shows the equivalent and actual damping ratio and right y-axis shows the magnification time r_m.

After obtaining the optimal analytical solutions for undamped structure, the one for damped structure can be directly obtained through Eq. (8) and (11). To minimize the error between the results of analysis formula and the exact values acquired by numerical method, the constant should be chosen as $\Omega = -\pi/2$. Here the Coe in ξ_d^{opt} is adjusted as Coe^n for a better accuracy and the factor n are 1 and 4 for γ^{opt} and ξ_d^{opt}, respectively, by try and error method. Then the solutions for damped structure are given by

$$\left.\begin{aligned} \gamma^{opt} &= \frac{\sqrt{1-\mu/2}}{\sqrt{1+\frac{4}{\pi^2}\xi_s^2}-\frac{2}{\pi}\xi_s}, & \xi_d^{opt} &= \frac{\sqrt{\frac{\mu^3(1-\mu/4)}{4(\mu^2-\mu+1)}}}{\left(\sqrt{1+\frac{4}{\pi^2}\xi_s^2}-\frac{2}{\pi}\xi_s\right)^4}, \text{ when } \mu<2 \\ \gamma^{opt} &= 0, & \xi_d^{opt} &= \frac{\sqrt{\frac{\mu^2}{4(\mu^2-\mu+1)}}}{\left(\sqrt{1+\frac{4}{\pi^2}\xi_s^2}-\frac{2}{\pi}\xi_s\right)^4}, \text{ when } \mu\geqslant 2 \end{aligned}\right\} \tag{28}$$

If $\xi_s = 0$, Eq. (28) will be reduced into Eq. (24) which for undamped case, therefore it is a general expression and works in both damped and undamped cases. In addition, the optimal performance index I^{opt} and equivalent damping ratio ξ_{se} for damped case can also be obtained by substituting Eq. (28) into (22) and (27), respectively.

Using numerical search method shown in Appendix A, we found that the influence of the damping ratio to TID performance is much less than that of the tuning ratio. Thus, a carefully tailed tuning ratio is of great importance.

3 The simplified design for the MDOF structure

To suppress the dynamic response of a complex MDOF structure, here an optimal design of TID targeting one modal of MDOF structure is considered. In MDOF structure, a TID can be installed between adjacent floors or between ground and 1^{st} storey to suppress vibration of primary structure. Thus compared to SDOF case, there is another design parameter, the installation location of TID, to be determined. The design is based on the concept that a specific vibration mode of a TID controlled MDOF structure can be replaced by an equivalent SDOF structure-TID system possessing the equivalent modal mass, stiffness and modal damping ratio. Consequently, the Eq. (28) which obtained by equivalent linearization method for SDOF structure-TID damped system can be used to calculate tuning ratio and damping ratio of the equivalent damped SDOF structure-TID system.

Firstly an n-storey building model subjected to ground motion excitation (in fact, it is readily to prove that the conclusion is same when the excitation is other form) and a TID system is mounted between storeys $i-1^{th}$ and i^{th} is established as shown in Figure 7.

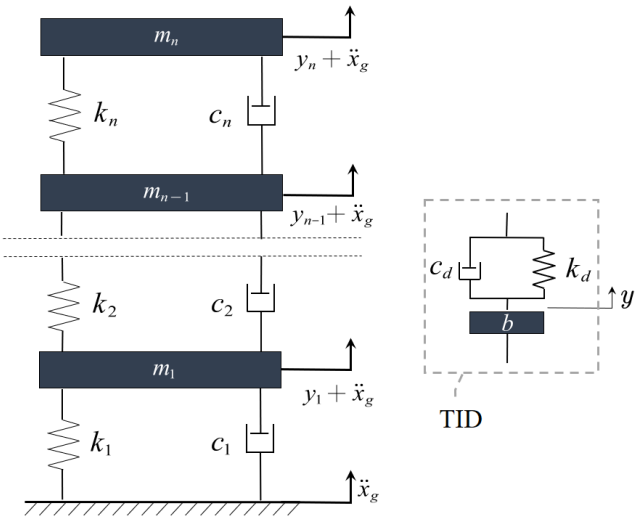

Figure 7 n-storey ground excited structure attached with a TID between storey $i-1$ and i.

The equation of motion of the combined system in Laplace domain is

$$[\mathrm{M}]s^2\{Y\}+[\mathrm{C}]s\{Y\}+[\mathrm{K}]\{Y\}=-[\mathrm{M}]\{I_n\}A_g+\{F_d\} \tag{29}$$

where $[\mathrm{M}]$, $[\mathrm{C}]$, and $[\mathrm{K}]$ denote the mass, damping, and stiffness matrices of the primary structure, respectively; $\{Y\}=\mathcal{L}(\{y\})=\{Y_1, Y_2, ..., Y_n\}$ is the Laplace transform of the relative displacement vector, where $\{y\}^T=\{y_1, y_2, ..., y_n\}$ is the displacement vector of primary structure relative to the ground; $\{I_n\}^T=\{1, 1, ..., 1\}$ is the unit vector; $A_g=\mathcal{L}(\ddot{x}_g)$ is the ground acceleration; $\{F_d\}$ is the vector of control force generated by the TID and equals to $\{w\}\{w\}^T W_d(s)\{Y\}$, where $W_d(s)$ is the ratio of the control force over the relative displacement $Y_{i-1}-Y_i$ of the two ends of TID as following

$$W_d(s)=\frac{s}{\frac{1}{\frac{k_d}{s}+c_d}+\frac{1}{bs}} \tag{30}$$

while $\{w\}$ is the control force position vector which has the form

$$\{w\}^T=\{0, \cdots, 0, -1, 1, 0, \cdots, 0\} \tag{31}$$

where the $(i\text{–}1)^{th}$ entry is -1 and the i^{th} entry is 1, meanwhile all the other entries are 0.

Then the displacement response $\{Y\}$ can be denoted in terms of modal vectors and coordinates

$$\{Y\}=[\Phi]\{Q\}=\sum_{i=1}^{n}\{\phi_i\}q_i \tag{32}$$

where $\{\phi_i\}^T=\{\phi_{1,i}, \phi_{2,i}, ..., \phi_{n,i}\}$ is the modal vector and $\{Q\}=\{q_1, q_2, ..., q_n\}$ is the modal coordinate vector. Substituting Eq. (32) into Eq. (29) and pre-multiplying both sides by $[\Phi]^T$, one obtains

$$[\mathrm{M}^*]s^2\{Q\}+[\mathrm{C}^*]s\{Q\}+[\mathrm{K}^*]\{Q\}=-[\Phi]^T[\mathrm{M}]\{I_n\}A_g-W_d[\Phi]^T\{w\}\{w\}^T[\Phi]\{Q\} \tag{33}$$

where $[\mathrm{M}^*]=[\Phi]^T[\mathrm{M}][\Phi], [\mathrm{C}^*]=[\Phi]^T[\mathrm{C}][\Phi], [\mathrm{K}^*]=[\Phi]^T[\mathrm{K}][\Phi]$ is the modal mass, damping, and stiffness matrix, respectively. Note that the matrix equation set Eq. (33) is coupled by the second term of the right side of equation. Yet when the excitation frequency ω close to the k^{th} natural frequency ω_k of the uncontrolled primary structure, the k^{th} modal response dominate. Based on this, it is reasonable to assume $\{Y\}\approx\{\phi_k\}q_k$. Then a set of uncoupled equations are obtained. The general form is as follow:

$$m_k^* q_k s^2+c_k^* q_k s+k_k^* q_k=-\{\phi_k\}^T[\mathrm{M}]\{I_n\}A_g-W_d(\phi_{i-1,k}-\phi_{i,k})^2 q_k \tag{34}$$

where m_k^*, c_k^*, k_k^* is the modal mass, damping, and stiffness, respectively. Note $\omega_k^2 = k_k^*/m_k^*$. Both displacements of two storeys where TID is mounted can also be approximate as

$$\left.\begin{array}{l} Y_{i-1} \approx \phi_{i-1,k} q_k \\ Y_i \approx \phi_{i,k} q_k \end{array}\right\} \tag{35}$$

Solving for q_k

$$q_k = \frac{Y_{i-1} - Y_i}{\phi_{i-1,k} - \phi_{i,k}} \tag{36}$$

Substituting Eq. (36) into Eq. (34) and rearranging the result, one obtains

$$m_{ke}^*(Y_{i-1} - Y_i)s^2 + c_{ke}^*(Y_{i-1} - Y_i)s + k_{ke}^*(Y_{i-1} - Y_i) = -m_{ke}^* \Xi_{ke} A_g - W_d(Y_{i-1} - Y_i) \tag{37}$$

This equation of motion is equivalent to that of a SDOF structure-TID system whose equivalent displacement of primary structure relative to ground is $Y_{i-1} - Y_i$; equivalent ground acceleration is $\Xi \ddot{x}_g$; and equivalent mass, damping, and stiffness etc. are

$$m_{ke}^* = \frac{m_k^*}{(\phi_{i-1,k} - \phi_{i,k})^2},\ c_{ke}^* = \frac{c_k^*}{(\phi_{i-1,k} - \phi_{i,k})^2},\ k_{ke}^* = \frac{k_k^*}{(\phi_{i-1,k} - \phi_{i,k})^2}, \Xi_{ke} = \frac{\phi_{i-1,k} - \phi_{i,k}}{m_{ke}^*} \{\phi_k^T\} [\mathrm{M}] \{I_n\} \tag{38}$$

Therefore the m_{ke}^*, c_{ke}^*, k_{ke}^* are also called equivalent modal mass, damping, and stiffness, respectively, for original MDOF structure. Note the modal damping ratio $\xi_k^* = c_k^*/(2m_k^* k_k^*)$ is not changes. Denoting the inertance to modal mass ratio as $\mu_k = b/m_k^*$, then the equivalent inertance to modal mass ratio is defined as

$$\mu_{ke} = \frac{b}{m_{ke}^*} = \mu_k (\phi_{i-1,k} - \phi_{i,k})^2 \tag{39}$$

This equation indicates that the inertance to modal mass ratio μ_k will be amplified when the MDOF structure-TID system is reduced to an equivalent SDOF one. The magnitude of the amplification factor , i.e. $(\phi_{i-1,k} - \phi_{i,k})^2$, is depending on the difference between two entries corresponding to the installation placement of TID in modal shape vector.

It have to note that the equation of motion Eq. (37) of the equivalent SDOF structure-TID system is not completely same with the general SDOF equation due to the terms Ξ_{ke} is not 1. Now the influence of Ξ_{ke} is discussed as following. Rearrange the Eq. (37) then the transfer function from ground acceleration $\Xi \ddot{x}_g$ to the equivalent displacement $\phi_{i-1,k} - \phi_{i,k}$ is given by

$$\frac{\phi_{i-1,k} - \phi_{i,k}}{A_g \Xi_{ke}} = \frac{-m_{ke}^*}{m_{ke}^* s^2 + c_{ke}^* s + k_{ke}^* + W_d} \tag{40}$$

where the Ξ_{ke} is a constant when the installation location of TID is certain. The right side of Eq. (40) is same with the transfer function of the SDOF system in form. Thus, the conclusion of SDOF system based on transfer function not be affected by Ξ_{ke} and can work directly here. As a result, If the μ_{ke} and ξ_k^* is given, the optimal tuning ratio and damping ratio of TID for k^{th} modal can be directly found using Eq. (28), the same is true for the optimal performance index and equivalent damping ratio. In addition, from the left side of Eq. (40), it emerges that Ξ_{ke} has influence on magnitude of response. This influence can also be expressed by q_k and μ_{ke} as following.

Combine Eq. (36), (38), (39), and (40) then the transform function form A_g to q_k can be obtained

$$\frac{q_k}{A_g} = \frac{-\{\phi_k\}^T [\mathrm{M}] \{I_n\}}{m_k^* s^2 + c_k^* s + k_k^* + \frac{W_d}{\mu_k} \mu_{ke}} \tag{41}$$

When excitation frequency ω close to the natural frequency ω_k and $c_k^* = 0$, the resonant modal response is

$$\frac{q_k}{A_g}(j\omega_k) = \frac{-\{\phi_k\}^T[\mathrm{M}]\{I_n\}\mu_k}{W_d\,\mu_{ke}} \tag{42}$$

It shows that the larger μ_{ke} will reduce the resonant modal response, so the optimal installation placement of TID for k^{th} modal can be preliminarily determined as the storey whose drift is maximum in modal shape, in other words, the i^{th} storey which can maximize the $(\phi_{i-1,k}-\phi_{i,k})^2$ is the optimal location.

Final, when a TID is installed in MDOF structure to suppress a specific vibration mode, the simplified design procedure can be summarized as follows:

Step 1. For the k^{th} vibration modal, first find the i^{th} story which corresponding to maximum $(\phi_{i-1,k}-\phi_{i,k})^2$ as the objective TID installation location.

Step 2. For a given inertance *b*, calculate the equivalent inertance to modal mass ratio μ_{ke} from Eq. (39) and then determine the modal damping ratio ξ_k^*. Note if the $\mu_{ke} > 1.28$, according to Figure 5 (b), the performance of TID will reduce. Thus, decrease the value of *b* so that $\mu_{ke} = 1.28$ is a good choice.

Step 3. Obtain the optimal tuning ratio γ^{opt} and damping ratio ξ_d^{opt} from Eq. (28) through substituting the μ and ξ_s by the μ_{ke} and ξ_k^*, respectively.

Step 4. Final the optimal stiffness and damping parameters can be obtained by

$$\left.\begin{aligned} k_d^{opt} &= b\gamma^2\omega_k^2 \\ c_d^{opt} &= 2\xi_{\mathrm{d}}\omega_k m_{ke}^* \end{aligned}\right\} \tag{43}$$

4 Comparison and validation of the proposed method

4.1 Accuracy validation

In previous section, a simplified design method is proposed for damped structures. Noting that the excitation is assumed as ideal white noise with uniform spectral density for all frequencies. Thus, the procedure is suitable for random excitation, that is, the excitation contains infinitely many frequencies. Whereas, if the excitation only contains few frequencies such as the harmonic, the proposed method is not suitable. To validate the closed-form formula proposed in section 2.2, a comparison between the proposed method and numerical search method is carried out. For numerical search method, the detailed procedure can be found at Appendix A. In addition, the values calculated by numerical method are identified as exact solution. All the solutions from two methods are listed in the Table 1. Please noting that these solutions

Table 1: The comparison of optimal tuning and damping ratios obtained from numerical search method and the proposed analytical method

μ	ξ_s	**Tuning ratio obtained numerically**	**Tuning ratio obtained analytically**	**Damping ratio obtained numerically**	**Damping ratio obtained analytically**
0.1	0.02	0.98387	0.98717	0.01696	0.01722
	0.04	0.99478	0.99982	0.01767	0.01812
	0.06	1.00755	1.01262	0.01850	0.01907
	0.08	1.02236	1.02558	0.01949	0.02006
	0.10	1.03946	1.03870	0.02066	0.02111
0.2	0.02	0.95981	0.96084	0.04981	0.05004
	0.04	0.97255	0.97315	0.05242	0.05266
	0.06	0.98705	0.98561	0.05545	0.05541
	0.08	1.00346	0.99823	0.05897	0.05830
	0.10	1.02196	1.01100	0.06304	0.06134
0.3	0.02	0.93349	0.93377	0.09355	0.09355
	0.04	0.94639	0.94573	0.09884	0.09843
	0.06	0.96069	0.95784	0.10481	0.10357

	0.08	0.97642	0.97010	0.11154	0.10898
	0.10	0.99353	0.98251	0.11902	0.11466
0.4	0.02	0.90537	0.90589	0.14490	0.14484
	0.04	0.91723	0.91749	0.15289	0.15241
	0.06	0.92992	0.92924	0.16159	0.16037
	0.08	0.94325	0.94114	0.17091	0.16874
	0.10	0.95692	0.95318	0.18069	0.17754
0.5	0.02	0.87556	0.87712	0.20033	0.20092
	0.04	0.88545	0.88836	0.21024	0.21141
	0.06	0.89543	0.89974	0.22048	0.22245
	0.08	0.90515	0.91125	0.23082	0.23406
	0.10	0.91417	0.92291	0.24092	0.24627

Table 1 shows the optimal tuning and damping ratios calculated by numerical and analytical , i.e. Eq. (28), methods in different particular pair of μ and ξ_s parameters, where $\mu \in [0.1:0.1:0.5]$ and $\xi_s \in [0.02:0.02:0.1]$. It emerges that the analytical and numerical results are in good agreement even the μ and ξ_s are larger. In addition, the relative errors between two results are plotted in following figure.

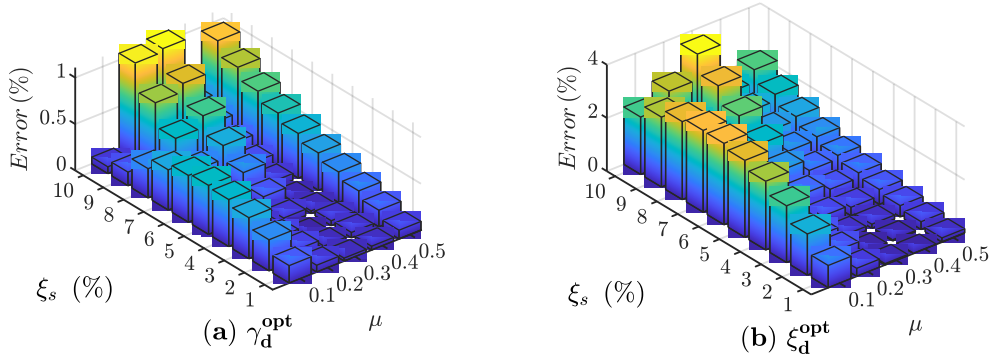

Figure 8 The relative errors between two methods against the inherent damping ratio ξ_s and inertance to mass ratio μ; (a) optimal tuning ratio, (b) optimal damping ratio.

As shown in Figure 8, the relative errors of two optimal solutions between numerical method and analytical method is very small. For optimal tuning ratio, the relative errors exceed 1 % slightly only when the $\xi_s = 0.1$. Although the maximum relative errors of damping ratio between numerical and analytical method is close to 4 %, the error is still acceptable because of the performance of optimization is insensitive to damping ratio ξ_s.

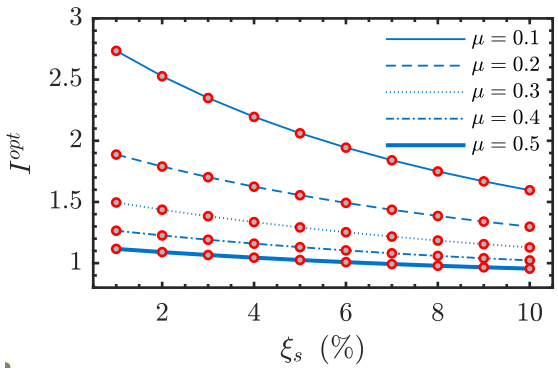

Figure 9 Comparison of the optimal performance index calculated by the analytical method (blue line) and numerical method (red points) for different inertance to mass ratio of TID and inherent damping ratio of the primary structure.

To further verify the effectiveness of the analytical method, Figure 9 shows the performance index I^{opt}

obtained from numerical and analytical method against the inherent damping ratio $\bar{\xi}_s$. It can be seen that the blue lines (denote the analytical method) almost coincide with the red points (denote the numerical method) over a large range of ξ_d and μ. In fact, the maximum relative errors of I^{opt} between two methods is only 0.037 %. It indicates that the analytical method has the same good control performance as the numerical method.

4.2 Method comparison when primary structure with uncertain parameters

In previous sections the parameters of primary structure are assumed to be determined. However, in practice primary structures are subjected to parametric uncertainty due to the damage of structures or error in measurement, etc. This section presents an investigation and comparison of the effects of the uncertainties in the primary structure parameters on the performance of the two design methods mentioned in section 4.1.

To investigate the parametric uncertainty, a Monte Carlo simulation for a structure with uncertain natural frequency and inherent damping ratio is carried out. In details, ω_s and ξ_s defined earlier are assumed as random independent variables which confirm to a normal distribution with a mean of $\bar{\omega}_s$ or $\bar{\xi}_s$ and a coefficient of variation of α. Then the Monte Carlo simulation is used to calculate the expected value of the performance index I defined in Eq. (21). A loss index is defined to denote the performance loss of TID due to the parametric uncertainty in primary structure and its form is

$$R = \frac{I_{opt}}{E(I)} \tag{44}$$

where I_{opt} is the performance index of system with certain parameters $\bar{\omega}_s$ and $\bar{\xi}_s$, and $E(I)$ is the expected value of the performance index of system with uncertain parameters ω_s and ξ_s. Theoretically, the R is less than one, i.e. $E(I) > I_{opt}$, because the increase of response due to the performance loss.

The TID-structure system in Figure 3 considering the parametric uncertainty is used as analysis model. For primary structure, 10000 random variables are generated for each parameter. The mean value of normal distribution are $\bar{\omega}_s = 2.5$ Hz and $\bar{\xi}_s = 0.02,\ 0.05$. The coefficients of variation are $\alpha = 0.1,\ 0.2,\ 0.3$ and all parameters have the same α at the same time. For TID, the inertance to mass ratio are $\mu = 0.05:0.05:0.5$ and the optimal parameters are obtained for mean value of primary structure by the proposed method and numerical search method as shown in Table 1. Based on this, the loss index is re-denoted as R_{Pro} and R_{Num}.

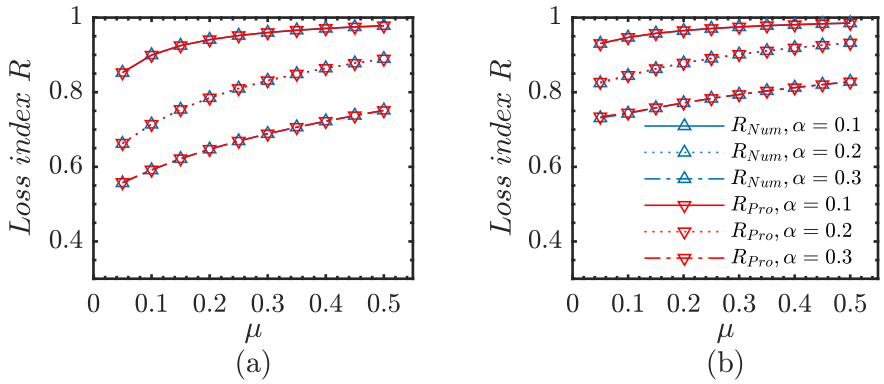

Figure 10 Comparison of performance between different optimal method: (a) $\bar{\xi}_s = 0.02$; (b) $\bar{\xi}_s = 0.05$

Figure 10 shows the comparison of two loss indices against the μ for different coefficients of variation. Two mean values of inherent damping ratio equal 0.02 and 0.05 are considered. The loss index R_{Pro} and R_{Num} are the same over the entire range. This illustrates the proposed method has the same robust performance with the numerical search method. In addition, it can be seen from Figure 10 (a) and (b) that the increase of robust performance of TID occur as the inertance to mass ratio μ increases, the coefficient of variation α decreases, and mean value of inherent damping ratio $\bar{\xi}_s$ increases.

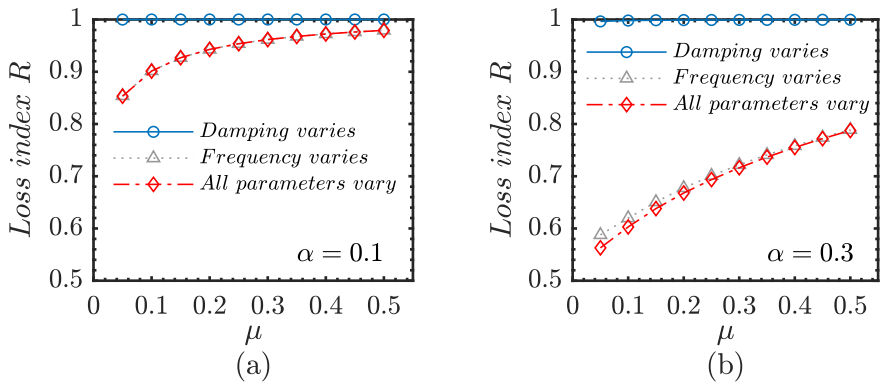

Figure 11 Comparison of relative effect of uncertainty in different parameters on TID performance, where $R = R_{Num}$, $\bar{\xi}_s = 0.02$; (a) $\alpha = 0.1$, (b) $\alpha = 0.3$.

Previous analysis is only based on the case that the uncertainty exists in all parameters. Now two new uncertainty cases are considered: uncertainty only in the natural frequency ω_s and uncertainty only in the inherent damping ratio ξ_s. Then the analysis of relative important of various uncertainty cases on TID performance are showed in Figure 11. It shows that the uncertainty in inherent damping ratio has very little effect on the TID performance. On the contrary, the effect on TID performance due to uncertainty in natural frequency is almost equal that considering uncertainty in all parameters. Besides, for high level of uncertainties the effect due to uncertainty in inherent damping ratio has a slight increase.

5 Case study

5.1 Numerical application

A 3-storey building model incorporating a TID system as shown in Figure 7 is used as example to investigate the feasibility of the simplified method proposed in this paper. Here b is considered as 500 kg. The building parameters are $m_1 = m_2 = m_3 = 1000$ kg and $k_1 = k_2 = k_3 = 1500$ kN/m. Then the modal shapes and natural frequencies are

$$\{\phi_1\} = \begin{bmatrix} 0.328 \\ 0.591 \\ 0.737 \end{bmatrix}; \{\phi_2\} = \begin{bmatrix} -0.737 \\ -0.328 \\ 0.591 \end{bmatrix}; \{\phi_3\} = \begin{bmatrix} 0.591 \\ -0.737 \\ 0.328 \end{bmatrix}; \tag{45}$$

$$\omega_1 = 17.236 \text{ rad/s}; \ \omega_2 = 48.296 \text{ rad/s}; \ \omega_3 = 69.789 \text{ rad/s}.$$

Consequently, the modal mass matrix is $[\mathrm{M}^*] = \mathrm{diag}\{1000, 1000, 1000\}\mathrm{kg}$ and the inertance to modal mass ratio μ_k for all three modal all equal to 0.5.

Now consider the optimal design of the 3-storey building-TID system by the simplified method. According to section 3, first the equivalent inertance to modal mass ratio μ_{ke} can be calculated by Eq. (39). Then the equivalent damping ratio provided by TID for one modal can be calculated by Eq. (27). For purpose of comparison, here all nine schemes, i.e., three installation locations for all three modes, are considered. All nine μ_{ke} and corresponding ξ_{se} are plotted in following figure.

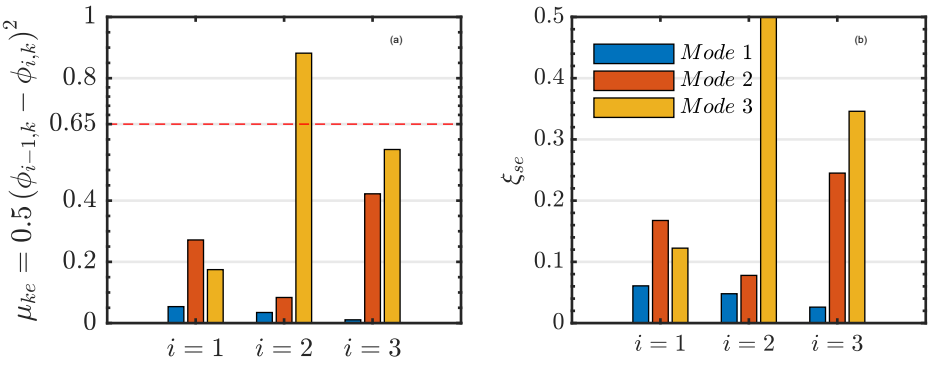

Figure 12 The relative influence of three installation locations of TID system on three modes; (a)

equivalent inertance to modal mass ratio against nine schemes, (b) equivalent damping ratio against nine schemes.

Figure 12 (a) shows all the nine μ_{ke}, and they equivalent damping ratios ξ_{se} calculated by Eq. (27) are plotted in Figure 12 (b). Please note, according to Figure 5 (b), the equivalent damping ratio achieves its maximum value 0.5 at $\mu = 0.65$ and only exists when $\mu \leqslant 0.65$. Thus, here for the scheme which TID mount at storey 2 and target the mode 3, the ξ_{se} cannot be calculated because its $\mu_{3e} = 0.88$. However, its equivalent damping ratio can be reasonably assumed as 0.5 in Figure 12 (b). Then from Figure 12 (b), the equivalent modal damping ratio provided by TID for each mode is different. The equivalent first modal damping ratio is always less than the second and third ones especially when TID is mounted at storey 2 and 3. This is because the shape of mode 2 and 3 are more curving than that of mode 1. Hence the amplification factor $(\phi_{i-1,k} - \phi_{i,k})^2$ of high-order modal is always larger than the low-order one (e.g., here $(\phi_{i-1,3} - \phi_{i,3})^2$ is always greater than $(\phi_{i-1,1} - \phi_{i,1})^2$). This is the source of the so-called high-order modal damping effect of TID [35][14][12][36]. Final. this figure intuitively depicts the optimal installation location for each modal. For example, for mode 1, mode 2, and mode 3, the optimal location is storey 1, storey 3, and storey 2, respectively. To verify this result, the mode 1 is considered to control. The design process is as following.

Following previous design procedure, the optimal tuning and damping ratio can be calculated by Eq. (28). Then according to Eq. (43), the optimal stiffness and damping quantities can be derived, the results are listed at following table.

Table 2: Optimal parameters of TID with different installation storey

Installation location	μ_{1e}	c_d(kNs/m)	k_d(kN/m)
Storey 1	0.0538	2.038	144.55
Storey 2	0.0346	1.624	145.98
Storey 3	0.0107	0.893	147.76

The history response curves and frequency spectrum of absolute acceleration of top storey when structure-TID system subjected to harmonic excitation with specific frequency are shown in Figure 13. From that it can be seen that the TID system with storey 1 installation have the best control performance for first modal response, while the response of TID mounted at storey 3 is maximal. It is not hard to conclude that the other modal control effects also conform to the conclusion in Figure 12. Thus, the effect of the design procedure is verified.

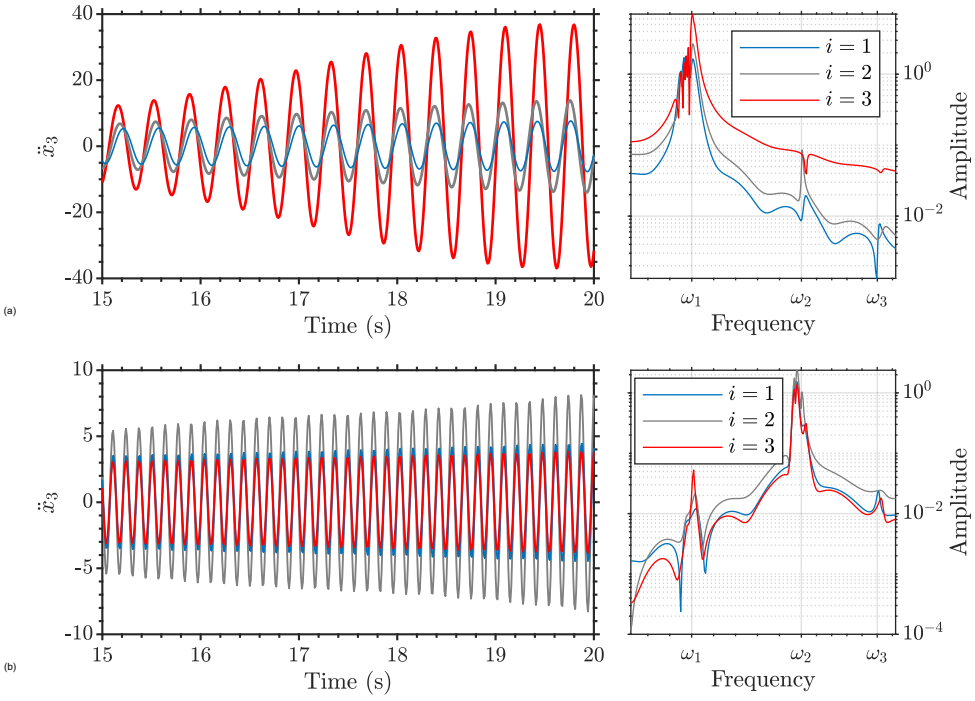

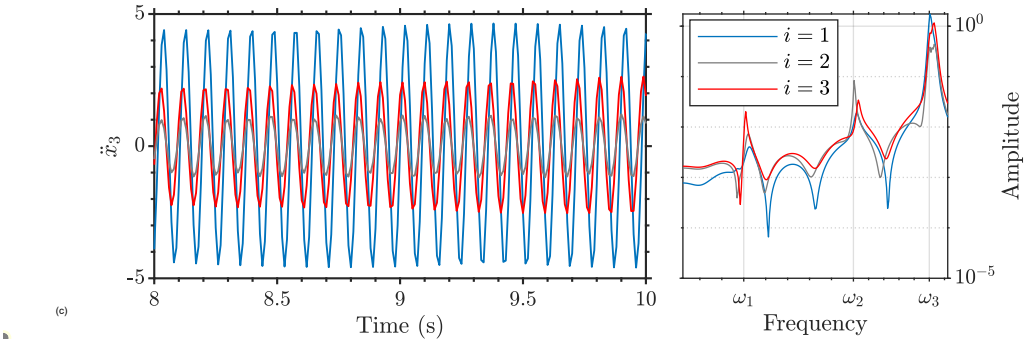

Figure 13 Harmonic responses in time and frequency domain of absolute acceleration of top storey considering three insaltallation locations of TID and excition frequency around (a) first natural frequency ω_1; (b) second natural frequency ω_2; (c) third natural frequency ω_3.

5.2 Seismic control performance

To investigate the performance of TID system in seismic control, the 3-DOF damped structure-TID system has been applied with earthquake excitations. In addition, the proposed method is compared with three optimization approaches, e.g., numerical approach 1 proposed by Lazar in [14], approach 2 with numerical optimization to minimize the floor acceleration and approach 3 with numerical optimization to minimize the storey drift. Note the latter two approaches uses the methodology presented in Appendix B with different objective functions (*OF*), i.e., minimizing floor acceleration or storey drift.

Here four practical earthquake records are selected as benchmark excitations: El Centro and Hachinohe as examples of far-field seismic motion, while Northridge and Kobe as examples of near-field seismic motion. Table 3 provides some detailed information on the earthquakes records.

Table 3: List of earthquakes considered in the numerical application

Earthquake	Date	Record location	Type	APA*
El Centro	May 18, 1940	Imperial Valley in El Centro,	Far-field	3.417
Hachinohe	May 16, 1968	Hachinohe City in Tokachi	Far-field	2.250
Northridge	Jan. 17, 1994	Los Angeles—UCLA Grounds	Near-field	8.266
Kobe	Jan.17, 1995	JMA station in Kobe, Japan	Near-field	8.178

Assume the structural damping to be proportional to stiffness as

$$[\mathbf{C}] = \alpha[\mathbf{K}] \tag{46}$$

where the constant α is defined as

$$\alpha = \frac{2\xi_i^*}{\omega_i} \ (i = 1, 2, 3) \tag{47}$$

in which ξ_i^* is the modal damping ratio of the i^{th} modal shape. We consider the fundamental modal to be controlled and assume $\xi_1^* = 0.02$, so one can derive that $\alpha = 2 \times 0.02/17.236 = 0.0023$. Then the structural inherent damping matrix and all modal damping ratios are described as follows

$$[\mathbf{C}] = \begin{bmatrix} 6.962 & -3.481 & 0 \\ -3.481 & 6.962 & -3.481 \\ 0 & -3.481 & 3.481 \end{bmatrix} \text{kNs/m}; \qquad \xi_1^* = 0.02; \quad \xi_2^* = 0.056; \quad \xi_3^* = 0.081. \tag{48}$$

Here it is obvious that the modal 1 is the control modal. According to the design procedure, the optimal parameters can be calculated by substituting $\mu = 0.0538$ and $\xi_s = 0.02$ into Eq. (28). In Table 4, results from Lazar's numerical approach 1, numerical approach 2, numerical approach 3 and the proposed approach in this paper are listed in term of optimal placement, system parameters, and performance

indices.

Table 4: Optimal parameters of TID by various optimization approach

Optimization approach	Optimal parameters		
	location	c_d (kNs/m)	k_d (kN/m)
Numerical approach 1 by Lazar[14]	Storey 1	2.5	138.6
Numerical approach 2	Storey 1	2.512	154.763
Numerical approach 3	Storey 1	1.846	133.050
The proposed approach	Storey 1	2.144	148.283

Two time history responses of system under representative EI Centro earthquake are used as example to illustrate the TID seismic control performance in Figure 14 and Figure 15. The proposed approach is compared with numerical approach 2 on acceleration response on top storey, and with numerical approach 3 on inter-storey drift response on bottom storey. It should note that the numerical approach 2 and numerical approach 3 respectively have the best performance on acceleration and drift response, respectively. In Figure 14, the reductions on peak acceleration relative to uncontrolled system of numerical approach 2 and the proposed approach are 36.474 % and 34.481 %, respectively. While for Figure 15, the reductions on peak inter-storey drift relative to uncontrolled system of numerical 3 and the proposed approach are 36.97 % and 36.36 %, respectively. From Figure 14 and Figure 15 it can be seen that both optimization methods show a good control effect and the response obtained by the proposed approach is similar to that obtained using numerical design procedure.

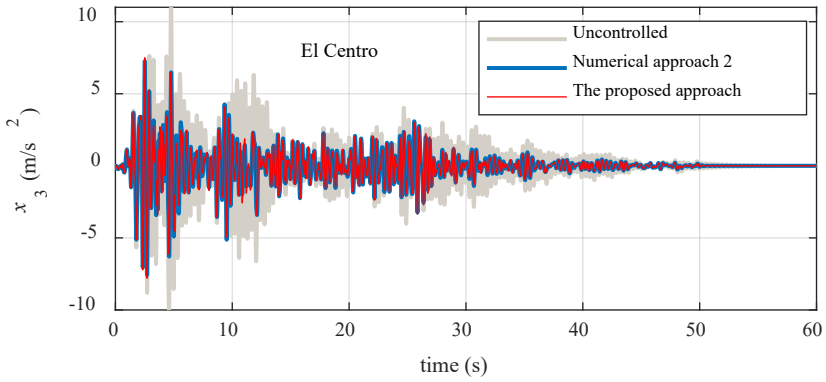

Figure 14 Time history of absolute acceleration response under El Centro earthquake for numerical acceleration optimization and analytical optimization

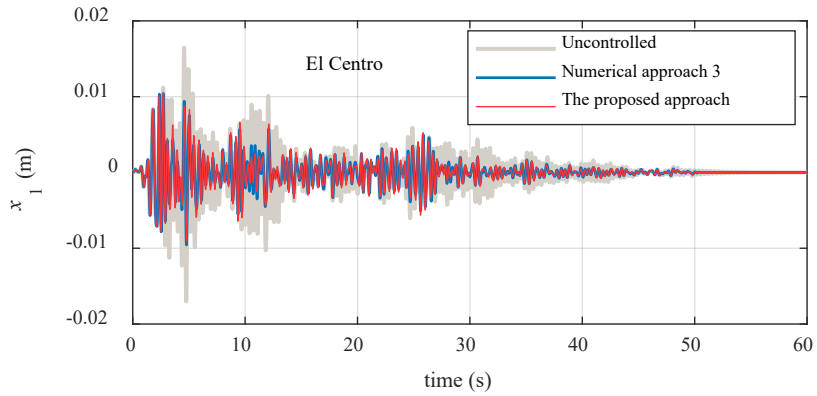

Figure 15 Time history of inter-storey drift response under El Centro earthquake for numerical drift optimization and analytical optimization

To show the interested responses of all the floors, all responses are calculated in terms of peak values and root mean square (RMS) values for all four earthquakes. Only the response profiles under Kobe earthquake excitation are plotted in Figure 16 and Figure 17 as a representative while others earthquakes responses are shown in Table 5 and Table 6. In a general view of the proposed method against all other proven approaches, it confirms that the proposed approach is able to achieve optimal design of TID for MDOF structure.

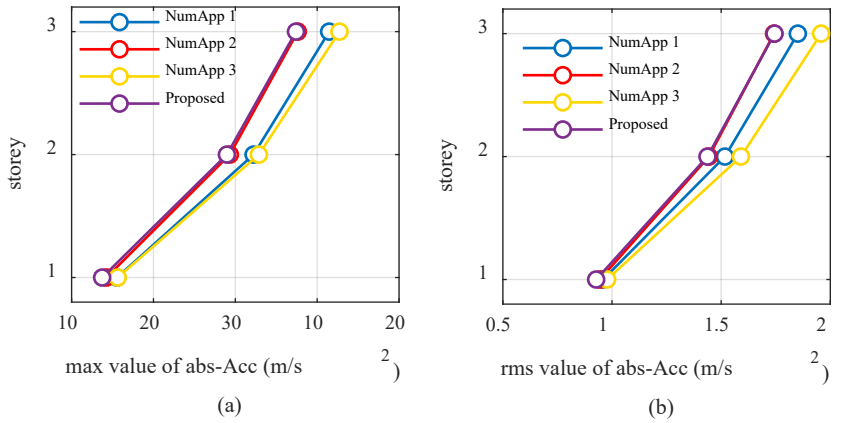

Figure 16 Storey absolute acceleration response in peak value form (a) and RMS value form (b) under Kobe earthquake

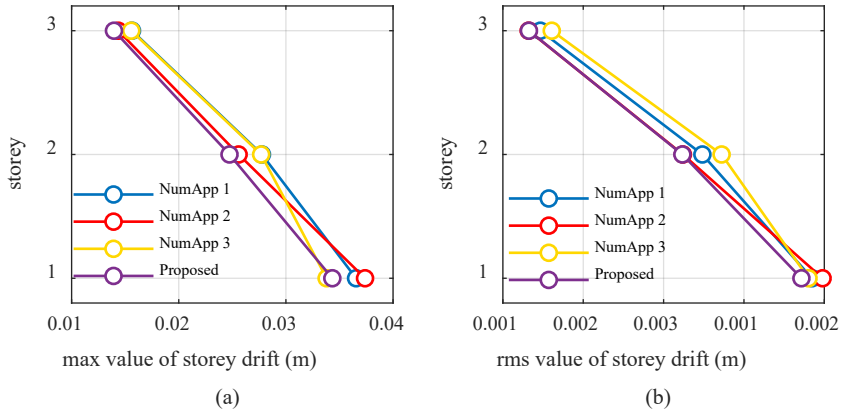

Figure 17 Storey inter-storey drift response in peak value form (a) and RMS value form (b) under Kobe earthquake

In Figure 16 the absolute acceleration on top storey for various optimization approaches are maximum meanwhile that responses on bottom storey are similar and relatively small, so the top storey should receive more attention in term of acceleration. The results in Figure 16 clearly show that the responses obtained by analytical and numerical acceleration optimization are similar and small enough than other two optimization methods. The results also show that the numerical drift optimization response is maximum. In storey drift response case as shown in Figure 17, unlike the acceleration case, the bottom storey response whatever the peak form or RMS form is maximum, however the top response is minimum. Thus the bottom storey should be considered as control implementation storey in storey drift optimization. In Figure 17 (a) it can be seen the numerical drift optimization response is minimum and the analytical optimization response is close but slightly larger, but on 2-storey and 3-storey, the analytical optimization response is minimum. The results also show that the numerical acceleration optimization response is maximum. In Figure 17 (b), similar results can be seen yet the bottom storey response are close to each other.

Table 5 Top storey acceleration response index under four earthquakes

	Numerical	**Analytical**

Earthquake excitation		Uncontrolled	Fixed-point by Lazar	Acceleration as objective	Storey drift as objective	Equivalent linearization method
El Centro	Peak	11.4368	7.2923	7.2653	7.5854	7.4933
	RMS	1.3865	0.8413	0.8473	0.8474	0.8411
Hachinohe	Peak	13.2460	6.6335	6.2211	7.1146	6.0693
	RMS	1.6623	0.7531	0.7287	0.7739	0.7250
Northridge	Peak	38.5638	32.7261	32.1234	32.9864	32.3597
	RMS	3.4523	1.9957	1.9665	2.0892	1.9883
Kobe	Peak	36.5941	25.7308	23.8145	26.3603	23.7050
	RMS	3.2608	1.8512	1.7423	1.9579	1.7445

Table 6 Bottom storey drift response index under four earthquakes

			Numerical			Analytical
Earthquake excitation		Uncontrolled	Fixed-point by Lazar	Acceleration as objective	Storey drift as objective	Equivalent linearization method
El Centro	Peak	1.65E-02	1.04E-02	1.05E-02	1.04E-02	1.05E-02
	RMS	2.11E-03	1.38E-03	1.46E-03	1.35E-03	1.42E-03
Hachinohe	Peak	1.97E-02	8.81E-03	8.57E-03	8.69E-03	8.29E-03
	RMS	2.50E-03	1.18E-03	1.24E-03	1.13E-03	1.18E-03
Northridge	Peak	5.44E-02	4.07E-02	4.19E-02	3.85E-02	4.03E-02
	RMS	5.18E-03	3.12E-03	3.33E-03	3.07E-03	3.22E-03
Kobe	Peak	5.82E-02	3.66E-02	3.74E-02	3.38E-02	3.43E-02
	RMS	4.91E-03	2.92E-03	2.99E-03	2.90E-03	2.86E-03

All response indices on key storeys under four earthquakes are shown in Table 5 and Table 6. It is clear that the TID system has excellent control performance. Furthermore, the effectiveness of the proposed analytical approach is proved since the results achieved by the proposed approach are very similar to that of complex numerical optimization. To add on, the analytical approach can better suppress the acceleration and storey drift response simultaneously while the numerical approaches 2 and 3 cannot. To summarize, the proposed approach has simple design procedure and the effect is convincing and satisfactory.

6 The Conclusions

This study aims to provide a simplified analytical approach to design the tuned inerter damper for seismic protection of both SDOF and MDOF damped structures. Determining the optimal design parameters (tuning ratio and damping ratio) and installation location of TID is the main objective of the TID design in this paper. A numerical approach also is developed as a reference for the analytical approach. The principal contributions of this research are as follow:

i. For damped SDOF structure, a closed-form formula based on equivalent linearization method is derived. The idea of this method is to replace the damped structure by an equivalent undamped structure. The proposed formula can obtain analytically both the tuning ratio and damping ratio of TID and the results are close to the exact solutions obtained by the numerical approach in Appendix A.

ii. For MDOF damped structure, a simple design procedure is proposed to obtain the design parameters of TID when targeting a modal. The method is based on the equivalent inertance to modal mass ratio μ_{ke} and the results of SDOF one can be used directly through μ_{ke}. An additional finding is that the high-order modal damping effect of TID is due to the curving shape of high-order modal shape. The method can also calculate the additional modal damping ratio provided by TID for a modal of MDOF structure and was confirmed by a 3-storey structure case study.

iii. A detailed procedure is proposed to design TID for suppressing the absolute acceleration response

or the inter-storey drift response of a MDOF damped structure considering the seismic excitations. The optimal design parameters and the optimal installation location of TID are determined numerically. The results show that the optimal installation location for both control objectives are all on the bottom storey.

iv. A numerical case study on the seismic performance of a three DOF structure considering four benchmark earthquakes as excitation are carried out finally. It is found that the proposed analytical approach achieves similar results compared with other proved numerical procedure. Thus the seismic performance of the proposed approach is satisfactory.

In conclusion, the proposed approach is proved valid in design of TID for both SDOF and MDOF damped structure. The advantages of its simple and convenient make it an attractive choice in engineering application.

Author contributions

T Xu: Conceptualization, Methodology, Formal analysis, Investigation, Writing – Original Draft, Writing – Reviewing and Editing, Visualization. Y Li: Conceptualization, Methodology, Supervision, Project Administration, Writing – Reviewing and Editing. T Lai: Writing – Reviewing and Editing. Jiajia Zheng: Writing – Reviewing and Editing.

Declaration of interest

The authors declare that they have no known competing financial interests or personal relationships that could have appeared to influence the work reported in this paper.

References

1. Smith MC. Synthesis of mechanical networks: The inerter【J】. *IEEE Transactions on Automatic Control* 2002; **47**(10): 1648–1662. DOI: 10.1109/TAC.2002.803532.
2. Chen MZQ, Papageorgiou C, Scheibe F, Wang FC, Smith M. The missing mechanical circuit element. *IEEE Circuits and Systems Magazine* 2009; **9**(1): 10–26. DOI: 10.1109/MCAS.2008.931738.
3. Smith MCAFCW. Performance Benefits in Passive Vehicle Suspensions Employing Inerters. *Vehicle System Dynamics* 2004; **42**(4): 235–257. DOI: 10.1109/ChiCC.2016.7554789.
4. Wang FC, Yu CH, Chang ML, Hsu M. The performance improvements of train suspension systems with inerters. *Proceedings of the IEEE Conference on Decision and Control* 2006: 1472–1477. DOI: 10.1109/cdc.2006.377606.
5. Ma R, Bi K, Hao H. A novel rotational inertia damper for heave motion suppression of semisubmersible platform in the shallow sea. *Structural Control and Health Monitoring* 2019; **26**(7): 1–24. DOI: 10.1002/stc.2368.
6. Ning D, Sun S, Du H, Li W, Zhang N, Zheng M, *et al.* An electromagnetic variable inertance device for seat suspension vibration control. *Mechanical Systems and Signal Processing* 2019; **133**: 106259. DOI: 10.1016/j.ymssp.2019.106259.
7. Hu Y, Chen MZQ, Smith MC. Natural frequency assignment for mass-chain systems with inerters. *Mechanical Systems and Signal Processing* 2018; **108**: 126–139. DOI: 10.1016/j.ymssp.2018.01.038.
8. Wang FC, Chen CW, Liao MK, Hong MF. Performance analyses of building suspension control with inerters. *Proceedings of the IEEE Conference on Decision and Control* 2007: 3786–3791. DOI: 10.1109/CDC.2007.4434186.
9. Ikago K, Sugimura Y, Saito K, Inoue N. Seismic displacement control of multiple-degree-of-freedom structures using tuned viscous mass dampers. *Proceedings of the 8th International Conference on Structural Dynamics, EURODYN 2011* 2011; **1**(3): 1800–1807.
10. Kohju Ikago KS and NI. Seismic control of single-degree-of-freedom structure using tuned viscous mass damper. *Earthquake Engineering and Structural Dynamics* 2012; **41**(3): 453–474. DOI: 10.1002/eqe.
11. Marian L, Giaralis A. Optimal design of a novel tuned mass-damper-inerter (TMDI) passive vibration control configuration for stochastically support-excited structural systems.

Probabilistic Engineering Mechanics 2014; **38**: 156–164. DOI: 10.1016/j.probengmech.2014.03.007.

12. Giaralis A, Petrini F. Wind-Induced Vibration Mitigation in Tall Buildings Using the Tuned Mass-Damper-Inerter. *Journal of Structural Engineering (United States)* 2017; **143**(9): 1–11. DOI: 10.1061/(ASCE)ST.1943-541X.0001863.

13. Siami A, Karimi HR, Cigada A, Zappa E, Sabbioni E. Parameter optimization of an inerter-based isolator for passive vibration control of Michelangelo's Rondanini Pietà. *Mechanical Systems and Signal Processing* 2018; **98**: 667–683. DOI: 10.1016/j.ymssp.2017.05.030.

14. I.F.Lazar, Neild SA, Wagg DJ. Using an inerter-based device for structural vibration suppression. *Earthquake Engineering and Structural Dynamics* 2014; **43**(8): 1129–1147.

15. Zhao G, Raze G, Paknejad A, Deraemaeker A, Kerschen G, Collette C. Active tuned inerter-damper for smart structures and its $\mathscr{H}\infty$ optimisation. *Mechanical Systems and Signal Processing* 2019; **129**: 470–478. DOI: 10.1016/j.ymssp.2019.04.044.

16. Gonzalez-Buelga A, Lazar IF, Jiang JZ, Neild SA, Inman DJ. Assessing the effect of nonlinearities on the performance of a tuned inerter damper. *Structural Control and Health Monitoring* 2017; **24**(3): 1–17. DOI: 10.1002/stc.1879.

17. Shen Y, Chen L, Yang X, Shi D, Yang J. Improved design of dynamic vibration absorber by using the inerter and its application in vehicle suspension. *Journal of Sound and Vibration* 2016; **361**: 148–158. DOI: 10.1016/j.jsv.2015.06.045.

18. Lazar IF, Neild SA, Wagg DJ. Performance analysis of cables with attached tuned-inerter-dampers. *Conference Proceedings of the Society for Experimental Mechanics Series* 2015; **2**: 433–441. DOI: 10.1007/978-3-319-15248-6_44.

19. Lazar IF, Neild SA, Wagg DJ. Vibration suppression of cables using tuned inerter dampers. *Engineering Structures* 2016; **122**: 62–71. DOI: 10.1016/j.engstruct.2016.04.017.

20. Sun H, Zuo L, Wang X, Peng J, Wang W. Exact H 2 optimal solutions to inerter-based isolation systems for building structures. *Structural Control and Health Monitoring* 2019; **26**(6): e2357. DOI: 10.1002/stc.2357.

21. De Domenico D, Impollonia N, Ricciardi G. Soil-dependent optimum design of a new passive vibration control system combining seismic base isolation with tuned inerter damper. *Soil Dynamics and Earthquake Engineering* 2018; **105**(September 2017): 37–53. DOI: 10.1016/j.soildyn.2017.11.023.

22. Krenk S, Hogsberg J. Tuned resonant mass or inerter-based absorbers: Unified calibration with quasi-dynamic flexibility and inertia correction. *Proceedings of the Royal Society A: Mathematical, Physical and Engineering Sciences* 2016; **472**(2185). DOI: 10.1098/rspa.2015.0718.

23. Hu Y, Chen MZQ, Shu Z, Huang L. Analysis and optimisation for inerter-based isolators via fixed-point theory and algebraic solution. *Journal of Sound and Vibration* 2015; **346**(1): 17–36. DOI: 10.1016/j.jsv.2015.02.041.

24. Shen W, Niyitangamahoro A, Feng Z, Zhu H. Tuned inerter dampers for civil structures subjected to earthquake ground motions: optimum design and seismic performance. *Engineering Structures* 2019; **198**: 109470. DOI: 10.1016/j.engstruct.2019.109470.

25. Wen Y, Chen Z, Hua X. Design and Evaluation of Tuned Inerter-Based Dampers for the Seismic Control of MDOF Structures. *Journal of Structural Engineering (United States)* 2017; **143**(4): 1–11. DOI: 10.1061/(ASCE)ST.1943-541X.0001680.

26. Pan C, Zhang R. Design of structure with inerter system based on stochastic response mitigation ratio. *Structural Control and Health Monitoring* 2018; **25**(6): 1–21. DOI: 10.1002/stc.2169.

27. Caughey T. Response of Van Der Pol's oscillator to random excitation. *Journal of Applied Mechanics* 1959; **26**(3): 345–348.

28. Caughey TK. Sinusoidal excitation of a system with bilinear hysteresis. *Journal of Applied Mechanics, Transactions ASME* 1960; **27**(4): 640–643. DOI: 10.1115/1.3644075.

29. Socha L, Soong TT. Linearization in analysis of nonlinear stochastic systems. *Applied Mechanics Reviews* 1991; **58**(1–6): 303–314. DOI: 10.1115/1.1995715.

30. Atalik TS, Utku S. Stochastic linearization of multi-degree-of-freedom non-linear systems. *Earthquake Engineering & Structural Dynamics* 1976; **4**(4): 411–420. DOI: 10.1002/eqe.4290040408.

31. N.D.Anh. Extension of equivalent linearization method to design ofTMD for linear damped systems. *Structural Control and Health Monitoring* 2012; **19**(6): 565–573. DOI: 10.1002/stc.446.

32. Anh ND, Nguyen NX. Design of TMD for damped linear structures using the dual criterion of equivalent linearization method. *International Journal of Mechanical Sciences* 2013; **77**: 164–170. DOI: 10.1016/j.ijmecsci.2013.09.014.

33. Asami T. Optimum Design of Dynamic Absorbers for a System Subjected to Random Excitation*. *JSME International Journal* 1991; **34**(2): 218–226.

34. Bakre S V., Jangid RS. Optimum parameters of tuned mass damper for damped main system. *Structural Control and Health Monitoring* 2007; **14**(3): 448–470. DOI: 10.1002/stc.166.

35. Giaralis A, Taflanidis AA. Reliability-based Design of Tuned Mass-Damper-Inerter (TMDI) Equipped Multi-storey Frame Buildings under Seismic Excitation. *In 12th International Conference on Applications of Statistics and Probability in Civil Engineering, ICASP 2015 University of British Columbia Library* 2015. DOI: 10.14288/1.0076257.

36. Giaralis A, Taflanidis AA. Optimal tuned mass-damper-inerter (TMDI) design for seismically excited MDOF structures with model uncertainties based on reliability criteria. *Structural Control and Health Monitoring* 2018; **25**(2): 1–22. DOI: 10.1002/stc.2082.

Appendix A: Numerical search method for SDOF system

In case of damped main structure (i.e. $\xi_s \neq 0$), the simultaneous equations Eq. (20) are very complex and cannot be solved analytically. Here we carry out a numerical approach to obtain directly the optimal parameters of TID for minimizing the performance index I.

The problem can be described as

$$\begin{gathered} for\ a\ given\ inertance\ b\ and\ \xi_s \\ find\ \gamma\ and\ \xi_d \\ minimizing\ the\ index\ I \\ subject\ to \begin{cases} 0<\gamma<\gamma_{\max} \\ 0<\xi_d<\xi_{d,\max} \end{cases}, \end{gathered}$$

where the lower bounds on γ and ξ_{d} are both zero and the above that are according to physical situation. The start points of γ and ξ_{d} are the results of Eq. (24).

The performance index i.e. H_2 norm, attains minimum value when the design parameters of TID system take the optimal values obtained from numerical technique. This can be verified by the fact that the optimal parameters curve is the lowest of all the curves in Figure . However, when the original configuration of structure changes because of structural damage or when we can only obtain the approximate solution calculated by analytical expression, it indicates that the design parameters are on detuning. Figure A depicts the detuning effect of tuning ratio γ and damping ratio ξ_{d} on the H_2 norm under different structural inherent damping ratio ξ_{s}, where various curves represent the TID parameters shift away from their respective optimal values in varying degrees. We can see that the H_2 norm increases considerably when tuning ratio γ deviates 20% from the optimal value, whereas the H_2 norm almost shows no increase even when the damping ratio ξ_{d} deviates 30% from the optimal value. This suggests that the performance of TID is far more sensitive to the γ than the ξ_{d}, in other words, the significance of accuracy of γ is more important than that of ξ_{d}.

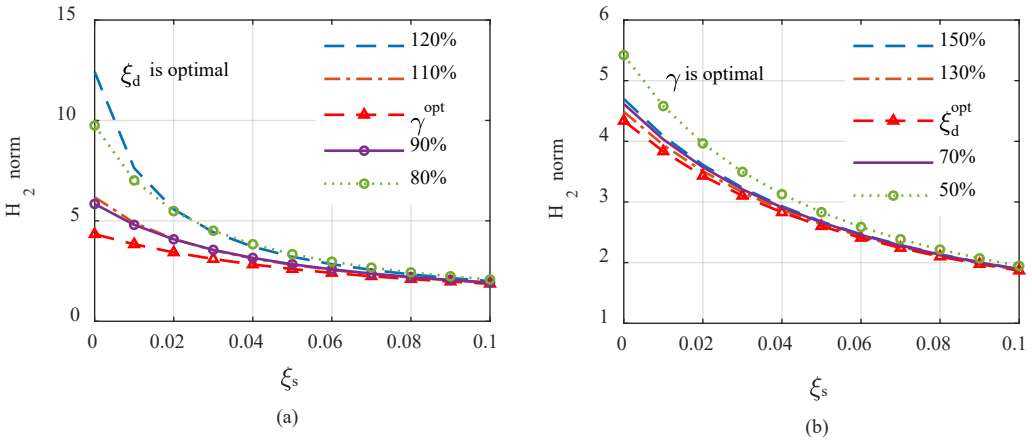

Figure A (a) detuning effect of tuning ratio γ on the H_2 norm. (b) detuning effect of damping ratio ξ_d on the H_2 norm.

Appendix B: Numerical search method for MDOF system

An *n*-storey structure subjected to ground motion is considered as the main structure, and a TID will be installed on certain storey as a control device. One of the most important aspect in various optimization strategies is the choice of the target response. Here we use the absolute acceleration or the storey drift response as objective of optimization because they are often primarily responsible for structural damage. The equation of motion in the Laplace domain of the system in Figure 7 is given by

$$\left([\mathbf{M}]s^2+[\mathbf{C}]s+[\mathbf{K}]\right)\tilde{\mathbf{X}}=\mathbf{P}_{eff}+\mathbf{F}_{\mathrm{con}}(s) \tag{B.1}$$

Where $[\mathbf{M}]$, $[\mathbf{K}]$ and $[\mathbf{C}]$ are, respectively, the mass, stiffness and damping matrices of primary structure; $\tilde{\mathbf{X}}=[\tilde{x}_1,\tilde{x}_2,...,\tilde{x}_{\mathrm{n}}]^T$ represents the Laplace transform of the structure response vector $\mathbf{X}=[x_1,x_2,...,x_{\mathrm{n}}]^T$ in time domain; $\mathbf{P}_{\mathrm{eff}}$ is the effective earthquake forces vector; $\mathbf{F}_{\mathrm{con}}$ is the TID control forces vector.

When the objective response is absolute acceleration of storey, the response x_{i} should be defined as the absolute displacement of the i^{th} storey, then the matrices in Eq. (B.1) are

$$\begin{gathered}[\mathbf{M}]=diag[m_1,m_2,...,m_{\mathrm{n}}];\\ [\mathbf{K}]=\begin{bmatrix}k_1+k_2 & -k_2 & \cdots & 0\\ -k_2 & k_2+k_3 & \cdots & \vdots\\ \vdots & \vdots & \ddots & -k_{\mathrm{n}}\\ 0 & \cdots & -k_{\mathrm{n}} & k_{\mathrm{n}}\end{bmatrix};\ [\mathbf{C}]=\begin{bmatrix}c_1+c_2 & -c_2 & \cdots & 0\\ -c_2 & c_2+c_3 & \cdots & \vdots\\ \vdots & \vdots & \ddots & -c_{\mathrm{n}}\\ 0 & \cdots & -c_{\mathrm{n}} & c_{\mathrm{n}}\end{bmatrix};\\ \mathbf{P}_{\mathrm{eff}}=\begin{bmatrix}c_1s+k_1\\ 0\\ \vdots\\ 0\end{bmatrix}\tilde{x}_{\mathrm{g}};\ \mathbf{F}_{\mathrm{con}}=\begin{bmatrix}-(l_1+l_2) & l_2 & \cdots & 0\\ l_2 & -(l_2+l_3) & \cdots & \cdots\\ \vdots & \vdots & \ddots & l_{\mathrm{n}}\\ 0 & \cdots & l_{\mathrm{n}} & -l_{\mathrm{n}}\end{bmatrix}W_{\mathrm{d}}\tilde{\mathbf{X}}+\begin{bmatrix}T_{\mathrm{d}}l_1\\ 0\\ \vdots\\ 0\end{bmatrix}\tilde{x}_{\mathrm{g}}.\end{gathered} \tag{B.2}$$

where m_{i} denote the lumped mass of i^{th} storey; c_{i} and k_{i} represent, respectively, the structure damping and stiffness between storeys $i-1$ and i; $\tilde{x}_{\mathrm{g}}$ is the Laplace transform of the ground displacement x_{g}; and W_d is defined at Eq. (30).

While the x_{i} is defined as the storey drift between storeys $i-1$ and i when the objective response is storey drift, note that x_1 denotes the displacement of 1^{st} floor relative to the ground, then these matrices become as follow

$$\begin{gathered}[\mathbf{M}]=\begin{bmatrix}m_1 & 0 & \cdots & 0\\ m_2 & m_2 & \cdots & 0\\ \vdots & \vdots & \ddots & \vdots\\ m_{\mathrm{n}} & m_{\mathrm{n}} & \cdots & m_{\mathrm{n}}\end{bmatrix};\ [\mathbf{C}]=\begin{bmatrix}c_1 & -c_2 & 0 & \cdots & 0\\ 0 & c_2 & -c_3 & \cdots & 0\\ 0 & 0 & c_3 & \ddots & \vdots\\ \vdots & \vdots & \vdots & \ddots & -c_n\\ 0 & 0 & 0 & 0 & c_n\end{bmatrix};\ [\mathbf{K}]=\begin{bmatrix}k_1 & -k_2 & 0 & \cdots & 0\\ 0 & k_2 & -k_3 & \cdots & 0\\ 0 & 0 & k_3 & \ddots & \vdots\\ \vdots & \vdots & \vdots & \ddots & -k_n\\ 0 & 0 & 0 & 0 & k_n\end{bmatrix};\\ \mathbf{P}_{\mathrm{eff}}=-\begin{bmatrix}m_1\\ m_2\\ \vdots\\ m_{\mathrm{n}}\end{bmatrix}\tilde{A}_{\mathrm{g}};\ \mathbf{F}_{\mathrm{con}}=\begin{bmatrix}-l_1 & l_2 & 0 & \cdots & 0\\ 0 & -l_2 & l_3 & \cdots & 0\\ 0 & 0 & -l_3 & \ddots & \vdots\\ \vdots & \vdots & \vdots & \ddots & l_n\\ 0 & 0 & 0 & 0 & -l_n\end{bmatrix}W_{\mathrm{d}}\tilde{\mathbf{X}}.\end{gathered} \tag{B.3}$$

where $\tilde{A}_{\mathrm{g}}$ represents the Laplace transfer of ground acceleration $\ddot{x}_{\mathrm{g}}$. Other parameters are the same as before.

Now the $\tilde{\mathbf{X}}$ can be obtained as the solution of Eq. (B.1), that is

$$\tilde{\mathbf{X}}=\left([\mathbf{M}]s^2+[\mathbf{C}]s+[\mathbf{K}]\right)^{-1}[\mathbf{P}_{eff}+\mathbf{F}_{\mathrm{con}}(s)] \tag{B.4}$$

and the transfer function from ground acceleration to structure response can be solved from Eq. (B.4)

$$TF(s)=\frac{\tilde{\mathbf{X}}}{\tilde{A}_{\mathrm{g}}}=\begin{bmatrix}\tilde{x}_1\\ \tilde{x}_2\\ \vdots\\ \tilde{x}_{\mathrm{n}}\end{bmatrix}/\tilde{A}_{\mathrm{g}}=\begin{bmatrix}TF_1\\ TF_2\\ \vdots\\ TF_{\mathrm{n}}\end{bmatrix} \tag{B.5}$$

where TF_{i} $(i=1,2,...,n)$ represents the transfer function from ground acceleration to response of i^{th} storey. The response vector $\tilde{\mathbf{X}}$ can denotes either absolute acceleration or storey drift response.

Now the objective function of numerical optimization can be defined as

$$OF(c_{\mathrm{d}},k_{\mathrm{d}},l_1,l_2,...,l_{\mathrm{n}})=max(I_{\mathrm{i}})\ (i=1,2,...,n) \tag{B.6}$$

where I_{i} is the H_2norm of transfer function TF_{i}, i.e. $I_{\mathrm{i}}=\frac{1}{2\pi}\int_{-\infty}^{\infty}|TF_{\mathrm{i}}(\omega)|^2 d\omega$, thus the objective function OF can automatic search for the key storey. then the numerical optimization problem is described as

$$\begin{gathered}for\ a\ given\ b\\ find\ optimal\ [l_1,l_2,...,l_{\mathrm{n}}],c_{\mathrm{d}}\ \&\ k_{\mathrm{d}}\\ minimizing\ OF\\ subjected\ to\begin{cases}0<c_{\mathrm{d}},0<k_{\mathrm{d}}\\ l_{\mathrm{i}}=1\ or\ 0,\ i=1,2,...,n\\ l_1+l_2+...+l_{\mathrm{n}}=1\end{cases}\end{gathered} \tag{B.7}$$